The Journal of Clinical Endocrinology & Metabolism, 2024, **00**, 1–11
https://doi.org/10.1210/clinem/dgae344
Advance access publication 16 May 2024
Clinical Research Article

Loading Enhances Glucose Uptake in Muscles, Bones, and Bone Marrow of Lower Extremities in Humans

Jakob Bellman,[1] Tanja Sjöros,[2,3] Daniel Hägg,[1] Erika Atencio Herre,[2,3] Janina Hieta,[4] Olli Eskola,[2] Kirsi Laitinen,[4] Pirjo Nuutila,[2,3,5] John-Olov Jansson,[1] Per-Anders Jansson,[6,7] Kari Kalliokoski,[2,3] Anne Roivainen,[2,3,8] and Claes Ohlsson[9,10]

[1]Department of Physiology, Institute of Neuroscience and Physiology, The Sahlgrenska Academy at the University of Gothenburg, SE-41390 Gothenburg, Sweden
[2]Turku PET Centre, University of Turku, FI-20014 Turun yliopisto, Finland
[3]Turku PET Centre, Turku University Hospital, FI-20520 Turku, Finland
[4]Nutrition and Food Research Center and Institute of Biomedicine, Integrative Physiology and Pharmacology Unit, Faculty of Medicine, University of Turku, FI-20014 Turun yliopisto, Finland
[5]Department of Endocrinology, Turku University Hospital, FI-20520 Turku, Finland
[6]Wallenberg Laboratory, Department of Molecular and Clinical Medicine, Institute of Medicine, Sahlgrenska Academy, University of Gothenburg, SE-41345 Gothenburg, Sweden
[7]Gothia Forum, Region Västra Götaland, Sahlgrenska University Hospital, SE-41346 Gothenburg, Sweden
[8]InFLAMES Research Flagship, University of Turku, FI-20014 Turku, Finland
[9]Sahlgrenska Osteoporosis Centre, Center for Bone and Arthritis Research, Institute of Medicine, Sahlgrenska Academy, University of Gothenburg, SE-41345 Gothenburg, Sweden
[10]Department of Drug Treatment, Region Västra Götaland, Sahlgrenska University Hospital, SE-41345 Gothenburg, Sweden

Correspondence: Claes Ohlsson, MD, PhD, Sahlgrenska University Hospital, Vita stråket 11, SE-41345 Gothenburg, Sweden. Email: claes.ohlsson@medic.gu.se.

Abstract

Context: Increased standing time has been associated with improved health, but the underlying mechanism is unclear.

Objectives: We herein investigate if increased weight loading increases energy demand and thereby glucose uptake (GU) locally in bone and/or muscle in the lower extremities.

Methods: In this single-center clinical trial with a randomized crossover design (ClinicalTrials.gov ID, NCT05443620), we enrolled 10 men with body mass index between 30 and 35 kg/m^2. Participants were treated with both high load (standing with weight vest weighing 11% of body weight) and no load (sitting) on the lower extremities. GU was measured using whole-body quantitative positron emission tomography/computed tomography imaging. The primary endpoint was the change in GU ratio between loaded bones (ie, femur and tibia) and nonloaded bones (ie, humerus).

Results: High load increased the GU ratio between lower and upper extremities in cortical diaphyseal bone (eg, femur/humerus ratio increased by 19%, $P = .029$), muscles (eg, m. quadriceps femoris/m. triceps brachii ratio increased by 28%, $P = .014$), and certain bone marrow regions (femur/humerus diaphyseal bone marrow region ratio increased by 17%, $P = .041$). Unexpectedly, we observed the highest GU in the bone marrow region of vertebral bodies, but its GU was not affected by high load.

Conclusion: Increased weight-bearing loading enhances GU in muscles, cortical bone, and bone marrow of the exposed lower extremities. This could be interpreted as increased local energy demand in bone and muscle caused by increased loading. The physiological importance of the increased local GU by static loading remains to be determined.

Key Words: positron emission tomography, PET/CT, whole-body imaging, obesity, energy metabolism, weight-bearing loading

Obesity is a growing problem worldwide, and related ailments, such as cardiovascular diseases and metabolic disorders, are major causes of death in the Western world (1). It has been demonstrated that increased standing time is associated with improved health outcomes such as reduced waist circumference, improved insulin sensitivity, and lower risk of developing obesity (2-4). Any causal relationship between standing time and reduced obesity is yet to be elucidated, but there is an ongoing discussion regarding posture allocation and its role in obesity (5).

The mechanisms for the potential health-promoting effects of standing are essentially unknown, but possible explanations could be static activation of postural muscles or increased weight-bearing loading. Recent studies suggest that the increased weight-bearing loading of the skeleton, which occurs during weight-bearing activities such as standing, can trigger a homeostatic body weight sensing system signaling from the bone to the brain, affecting energy balance (6, 7).

Our knowledge about the role of the human skeleton has evolved from mainly functioning as a structural frame to being

Received: 8 March 2024. **Editorial Decision:** 14 May 2024. **Corrected and Typeset:** 4 June 2024

considered an endocrine organ (8). It has been shown that weight-bearing exercise can increase bone mineral density and reduce fat mass, making it an important factor in the regulation of bone mass and energy consumption (9, 10). There is also evidence showing an interplay between bone and whole-body glucose homeostasis and that osteoblast lineage cells are involved in the regulation of glucose homeostasis (11). It is believed that not only bone cells but also bone marrow cells play a role in glucose homeostasis (12-15). The bone marrow is largely composed of the bone marrow adipose tissue (BMAT), which play an important role in whole-body energy homeostasis by secreting cytokines and adipokines (16, 17). Bone is increasingly recognized as an endocrine organ, but the knowledge of energy expenditure and glucose uptake (GU) in the human skeleton is limited.

Muscles have an important role in energy and glucose homeostasis, and studies have shown that exercise of muscles in the lower extremities increases GU not only in the exposed muscles but also in BMAT (18, 19). Whether standing with its corresponding increased static muscle activity and increased weight-bearing loading affect GU locally in muscles, adipose tissue, or bone is unknown. We hypothesize that increased weight-bearing loading increases energy consumption locally in tissues exposed to loading. Over time, increased weight-bearing loading could result in reduced fat mass and body weight, making it a potential treatment option for obesity. The aim of the present study was to investigate the effects of increased weight-bearing loading (applied using a weight vest) as compared to no load on GU locally in the exposed bones and muscles.

Materials and Methods

Study Design

This was a single-center interventional imaging crossover study (Weight Load PET, ClinicalTrials.gov ID, NCT05443620). The aim was to evaluate GU in different tissues after the treatment of standing with a heavyweight vest (= high load, 11% of body weight) compared to sitting (= no load). The loading method with heavyweight vests was based on a method from a previously published study (7). Beyond the screening visit, all participants took part in 2 separate visits: (1) high load visit (= standing with heavyweight vest) and (2) no load visit (= sitting in a wheelchair). The order of the visits was randomized using a Microsoft Excel randomization formula, and the visits took place approximately 1 to 3 weeks apart. The different interventions (1) and (2) were chosen to achieve as large a difference in axial loading on the lower extremities as possible between the study visits. Furthermore, participants with obesity were recruited to further increase the difference in axial, weight-bearing loading between treatments. The study was performed at Turku PET Centre, Turku University Hospital, Finland, in collaboration with researchers from the University of Gothenburg, Sweden. Participants were recruited using local advertisements, and potential participants were booked for a screening visit at the study center.

A total of 14 potential participants were screened, and 10 male adults completed the study (see Fig. 1) with baseline characteristics as described in Table 1. All participants signed written informed consent before participation. The study was performed according to the Declaration of Helsinki and was approved by the Ethical Committee of the Hospital District of Southwest Finland.

Participants

Men with obesity [body mass index (BMI) > 30 and ≤ 35 kg/m^2, fat mass > 25% of total body weight] between 18 and 65 years of age, with a maximum body weight of 115 kg, who were willing to comply with the study protocol, had normal or clinically nonsignificant aberrations of screening blood samples (blood cell count, electrolytes, liver function, hemoglobin A1c (HbA1c), plasma glucose, lipid profile, thyroid function, and C-reactive protein), and who signed informed consent were eligible for participation. The exclusion criteria were the following: chronic disease that could interfere with participation in the study as judged by the investigator, diabetes, chronic pain, consumption of medications affecting food intake or metabolism, bariatric metabolic surgery, reduced mobility, use of illegal drugs or nicotine products, use of excessive amounts of alcohol [>14 glasses of wine (15 cL/glass 11% alcohol)] per week or equivalent, change in body weight ≥5 kg during the last 3 months. Participants whose body weight changed more than 3 kg between screening and the following study visits, who had a drastic change in lifestyle with regards to dietary or physical activity habits as judged by the investigator, or had a risk of not being able to comply with the study protocol as judged by the investigator were excluded from the analyses.

Enrollment

Potential participants were booked for a screening visit where signed informed consents for participation in the study were collected and the participants were checked for compliance with the eligibility criteria. Body weight at screening and other visits was measured using a calibrated scale [Seca scales (ref. I110785), Seca, Germany]. Fat mass and fat-free mass were measured with air displacement plethysmography and an electronic scale (the Bod Pod system, COSMED, Inc., Concord, CA, USA). Height was measured for BMI calculation. Participants underwent an orthostatic blood pressure test using calibrated standard equipment for every measurement (Apteq or Omron Intellisense blood pressure machine). All blood samples were analyzed at the local hospital-certified laboratory. Enrollment and study flow are shown in Fig. 1.

Participant Preparation

Participants were instructed to continue with their habitual lifestyle during their participation in the study. Forty-eight hours before each visit, participants were instructed to refrain from exhaustive physical activity, sauna, and alcohol. Twenty-four hours before each visit, they were instructed to refrain from caffeine-containing beverages. They had an overnight fast (>8 hours) from the evening before each visit. Three hours before each visit, participants completed a standardized breakfast [80 g oatmeal porridge, 200 mL milk (1.5% fat), 200 mL juice, 1 banana, and 200 mL yoghurt (2% fat); 544 kcal, including protein 11.8 E%, carbohydrates 70.1 E%, fat 14.3 E%] followed by another 3-hour fasting period before the visit start. Fasting was then maintained during the study visits, but intake of water was allowed after body weight measurements at the start of each visit.

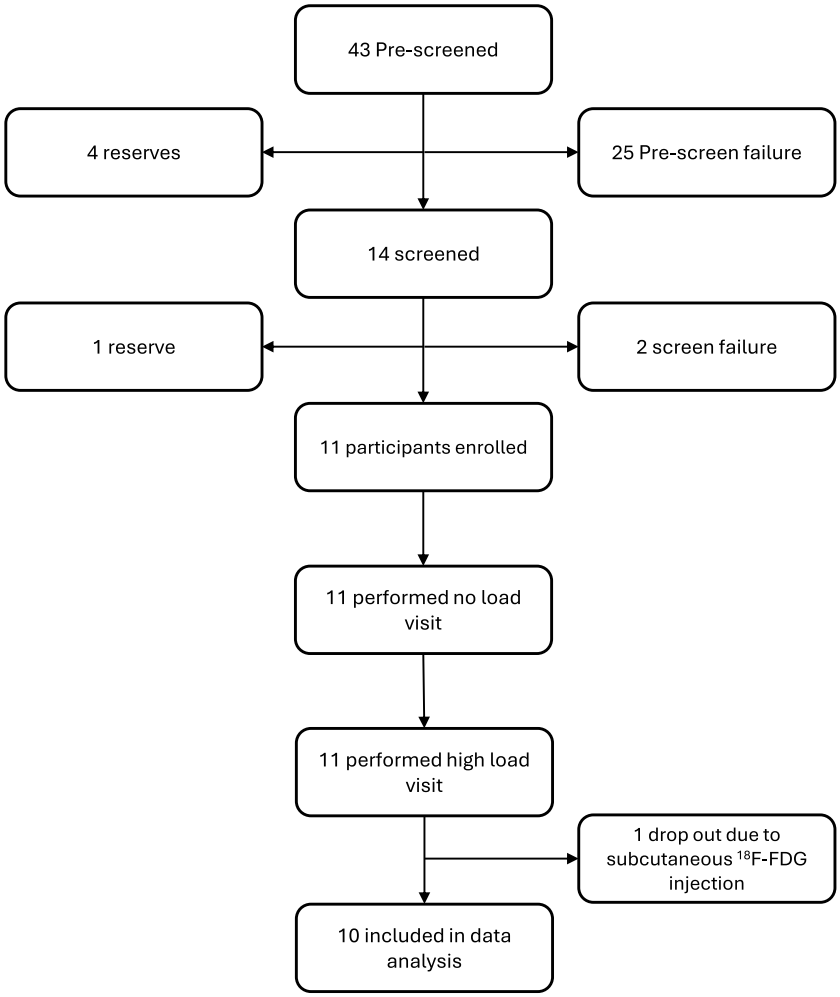

Figure 1. CONSORT diagram describing enrollment and study flow. The participants with screening failure did not meet all inclusion criteria and/or did meet at least 1 of the exclusion criteria as described in Methods.

Experimental Protocol

A schematic diagram of experimental protocol is shown in Fig. 2. Study visits started with a weighing followed by a 1-hour resting period in the supine position. Then participants changed position to either (1 = high load) standing or (2 = no load) sitting in a wheelchair. During visit (1) participants put on a heavyweight vest (PRF Weight Vest, Casall, Norrköping, Sweden) consisting of 11% of the participants' body weight, and during visit (2) participants sat in the wheelchair without a vest with their feet on the footrests. The participants held this position for a total of 3 hours and were instructed to be completely still and to distribute their body weight evenly on both lower extremities. They were not allowed to lean toward or rest their arms on any surface during the experiment. To reduce strain and discomfort, they performed a 2.5-minute slow-paced walk every 30 minutes during the first 105 minutes. Walking was performed on a flat surface with no in- or decline. After each walk, the participant returned to the original position. After 105 minutes, no further movement was allowed. The same movement schedule was followed at the (2) no load visit but participants then moved in their wheelchair on a flat surface using their arms without applying pressure on their feet.

Fluorine-18 labeled glucose analog, 2-deoxy-2-[^{18}F]-fluoro-D-glucose (^{18}F-FDG; mean dose 102.7 MBq, SD ± 4.0) was used as a radiopharmaceutical and was injected at 120 minutes after a 6-hour fasting period while the participants remained in the allocated position. At 180 minutes, participants were moved in a wheelchair [also after the (1) high load treatment] to the scanner room to perform a whole-body quantitative positron emission tomography/computed tomography (PET/CT). During the (1) high load visit, the weight vest was removed immediately before scanning started. The PET/CT method used in this study evaluated GU in different tissues during the treatments even though the measurement was performed immediately after the treatment, since a majority of the cellular ^{18}F-FDG uptake takes place in the first minutes after injection. The glucose analogues were then trapped intracellularly enabling a subsequent PET/CT scan that still measured GU during and not after the treatment (20).

PET/CT Image Acquisition

The participants were positioned supine in the scanner. A long axial field-of-view Biograph Vision Quadra (Siemens Healthcare GmbH, Munich, Germany) PET/CT device was used to scan the whole body. CT scans were performed with a slice thickness of 1.5 mm, pitch factor 1.7, 120 kV, and 9 mAs. PET data were acquired in a list mode for using 2 bed position (10 minutes each) with a field of view of

Table 1. Clinical characteristics from screening for all men included in the analysis

Anthropometry	Mean	± SD	n
Age (years)	38.4	7.9	10
Height (cm)	182	6.7	10
Weight (kg)	106.2	7.6	10
BMI (kg/m^2)	32.2	2.1	10
Fat percent (%)	36.6	3.9	10
Fat mass (kg)	38.9	5.3	10
Fat-free mass (kg)	67.2	5.9	10
Plasma markers			
Total cholesterol (mmol/L)	4.9	0.7	10
HDL cholesterol (mmol/L)	1.1	0.2	10
LDL cholesterol (mmol/L)	3.2	0.6	10
Fasting triglycerides (mmol/L)	1.6	0.8	10
Fasting insulin (mU/L)	16.1	6.8	10
HOMA-IR index	4.2	1.9	10
Fasting plasma glucose (mmol/L)	5.7	0.4	10
CRP (mg/L)	5.0	7.3	10
ALT (U/L)	59.4	31.6	10
AST (U/L)	34.2	10.8	10
ALP (U/L)	64.1	11.0	10
TSH (mU/L)	1.8	0.5	10
Thyroxine (pmol/L)	15.7	1.5	10
Blood markers			
Red blood cells (10^{12}/L)	5.2	0.4	10
White blood cells (10^9/L)	6.4	1.3	10
Hemoglobin (g/L)	161.0	10.6	10
Platelets (10^9/L)	256.9	44.9	10
HbA1c (mmol/mol)	35.6	3.0	8
HbA1c (%)	5.4	0.7	8

Data are expressed as mean ± SD.
Abbreviations: ALT, alanine transaminase; ALP, alkaline phosphatase; AST, aspartate transaminase; BMI, body mass index; CRP, C-reactive protein; HbA1c, hemoglobin A1c; HDL, high-density lipoprotein; HOMA-IR, homeostatic model assessment for insulin resistance; LDL, low-density lipoprotein.

106 cm. PET data were corrected for attenuation, randoms, scatter, and decay and reconstructed with the vendor's time of flight point-spread-function algorithm with 4 iterations and 5 subsets. The resulting image size was $440 \times 440 \times 425$ with a voxel size of $1.65 \times 1.65 \times 2.50$ mm^3. The input function for the quantification of PET image data was obtained from repeated arterialized venous blood samples taken from the tracer injection until the end of the PET scans. The radioactivity concentration in the plasma was measured with a gamma counter (AMG, Hidex, Turku, Finland) cross-calibrated with the dose calibrator (VDC-202; Veenstra Instruments, Joure, the Netherlands) and the PET/CT scanner. CT images obtained from the same scanning session were used for anatomical reference.

Image Analysis

PET images were corrected for decay and quantification of ^{18}F-FDG uptake was performed by standard region of interest (ROI) analysis followed by the calculation of the fractional uptake rate (FUR) using the PET image data and the individual input function, ie, plasma radioactivity data (21, 22).

The ROIs were defined on targeted tissues on 5 adjacent PET image slices (each slice approximately 3 mm thick) on the transverse plane analyzing specific sections of each tissue. The Carimas Research v2.10 software (Turku PET Centre, University of Turku, Finland) was used to define ROIs, and the definitions for each specific tissue were all made by 1 investigator to avoid interobserver differences. Glucose FUR values were obtained for the following tissues:

- Cortical bone
  - Diaphyseal part of femur, tibia, and humerus.
- Bone marrow region
  - Diaphyseal part of femur, tibia, and humerus.
  - Vertebral bodies of Th10-Th12 and L3-L4.
- Muscles
  - Quadriceps femoris muscle, triceps surae muscle, triceps brachii muscle.
- Adipose tissue
  - Visceral adipose tissue at L3-L4 level.
  - Subcutaneous adipose tissue (SAT) in femoral, tibial, and humeral regions. SAT also analyzed in ventral part of abdominal area at L3-L4 level.
  - Supraclavicular brown adipose tissue (BAT).

For all ROIs in extremities, bilateral glucose FUR values (mean values in both legs and both arms) were used in the analysis. An illustration of the ROI drawing is shown in Fig. 3. Glucose FUR values were further converted into glucose uptake values using the following formula:

$$Glucose\ Uptake\left(\frac{\mu mol}{kg\ x\ min}\right) = \frac{FUR\ x\ Plasma\ Glucose}{Lumped\ Constant\ x\ Tissue\ Density}$$

Plasma glucose levels were obtained from plasma sampling during the visits and calculated as the mean of the plasma glucose values taken at 120 minutes and onwards, values from the ^{18}F-FDG injection until the end of the experiment. The lumped constant (LC) is a value that considers differences in the uptake of glucose and ^{18}F-FDG from the blood to different tissues. For muscle it is 1.16 and for adipose tissue 1.14 (23, 24). There is no calculated LC for other analyzed tissues; thus the LC for those tissues has been assumed to be 1. Tissue density was acquired from the Report of the Task Group on Reference Man (25).

Blood Sampling and Vital Signs

At the start of each visit, 2 Teflon catheters were inserted into the antecubital veins on each forearm of the volunteer: 1 for an injection of ^{18}F-FDG and the other for blood sampling. Arterialized venous blood samples for measurement of plasma radioactivity concentration were obtained repeatedly starting from the tracer injection and ending at the end of the PET scans for each study visit separately. Plasma glucose samples were collected from −30 minutes and then every 30 minutes until the end of the visit. Plasma insulin, free fatty acids, and lactate samples were collected at −30, 0, 60, 120, and 180 minutes. All samples were analyzed in the certified local laboratory at

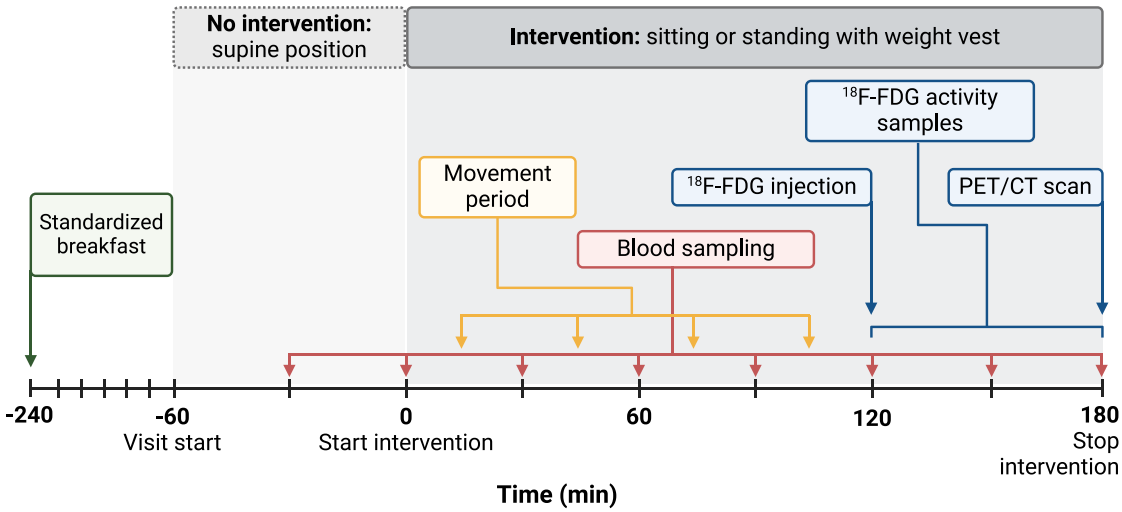

Figure 2. Schematic diagram of experimental protocol. After 3 hours of intervention, each visit ended with a whole-body PET/CT scan. Three hours before each study visit, participants consumed a standardized breakfast. During the intervention, there were 4 short movement breaks (orange box and arrows). Blood samples were collected at several timepoints from −30 minutes to 180 minutes according to the description in Methods (red box and arrows). At 120 minutes, ^{18}F-FDG was injected followed by radioactivity blood sampling from 120 to 180 minutes and finally a whole-body PET/CT at 180 minutes (blue boxes, arrows, and bracket). Created with publication rights from BioRender.com.

Abbreviations: ^{18}F-FDG, 2-deoxy-2-[^{18}F]-fluoro-D-glucose; PET/CT, positron emission tomography/computed tomography.

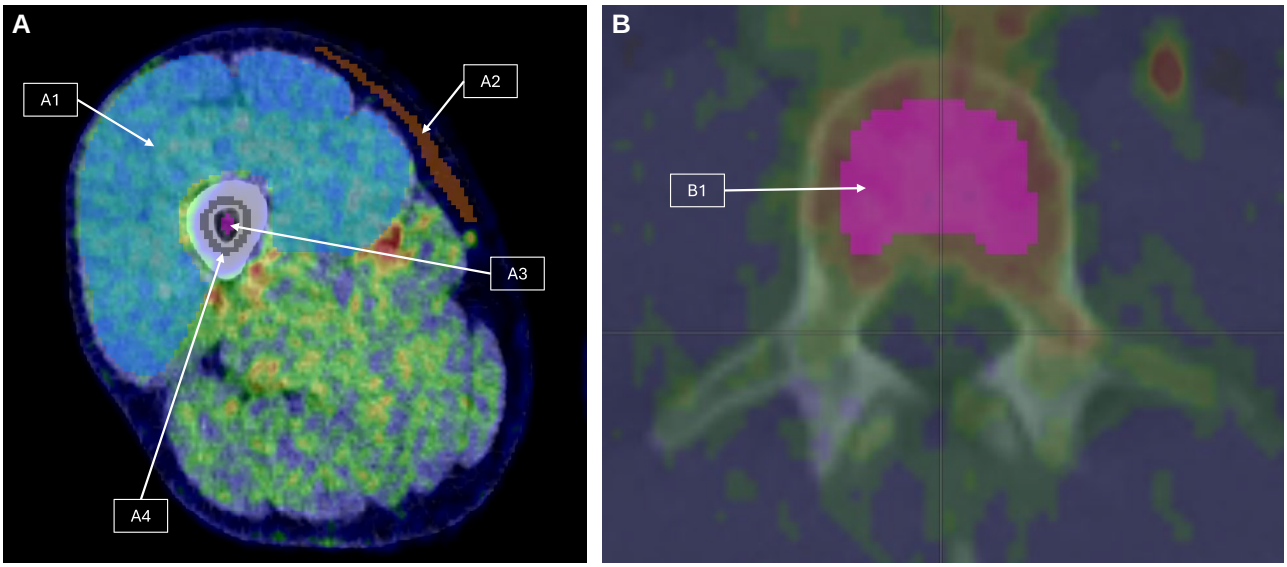

Figure 3. Images from a participant's (A) right lower extremity and (B) lumbar vertebrae L3. (A) Shows a transversal plane PET/CT section with ROI drawing on (A1) quadriceps muscle, (A2) subcutaneous adipose tissue in femoral region, (A3) femoral diaphyseal bone marrow cavity, and (A4) cortical femoral bone. (B) Shows a transversal plane PET/CT section with ROI drawn on the vertebral body (B1) on the L3 vertebrae.

Abbreviations: PET/CT, positron emission tomography/computed tomography; ROI, region of interest.

Turku University Hospital, Turku, Finland, using standardized procedures. Plasma insulin, TSH, and free T4 were determined by electrochemiluminescence immunoassay (TSH, RRID:AB_2756377; T4, RRID:AB_2756378; insulin, RRID:AB_2756877) and C-reactive protein by immunoturbidimetry (Cobas 8000 e801, Roche Diagnostics GmbH, Mannheim, Germany, RRID:SCR_025257). Plasma glucose was determined by an enzymatic reference method with hexokinase GLUC3; plasma triglycerides, cholesterols (total, low-density lipoprotein, high-density lipoprotein), and free fatty acids by enzymatic colorimetric tests; lactate by an enzymatic reference method; and alanine transaminase, aspartate transaminase, alkaline phosphatase by kinetic photometry (Cobas 8000 c702, Roche Diagnostics GmbH, RRID:SCR_025256). HbA1c was determined by turbidimetric inhibition immunoassay (Cobas 6000 c501, Roche Diagnostics GmbH, RRID:SCR_025255; immunoassay, RRID:AB_2909460). Percentage HbA1c was calculated using the formula: HbA1C (%) = [HbA1c (mmol/mol)/10.929] + 2.15 (26). The homeostatic model assessment for insulin resistance index was calculated by the following formula: fasting glucose (mmol/L) × fasting insulin (mU/L)/22.5 (27). Pulse rate and blood pressure were measured at both visits at 0, 90, and 180 minutes.

Outcomes

GU ratios were calculated in weight-loaded regions (ie, lower extremity) compared to nonweight-loaded regions (ie, upper extremity). The predefined primary endpoint was the change in this GU ratio in cortical bone between (1) high load (standing with a weight vest weighing 11% of the participant's body weight) and (2) no load (sitting in a wheelchair without a vest). Main secondary endpoints included change in the same ratio for (1) diaphyseal bone marrow region, (2) muscles, and (3) SAT in high load compared to no load. Secondary endpoints also included absolute changes in GU, not adjusted for GU uptake in upper extremities, in the aforementioned tissues.

Key exploratory endpoints were absolute changes in GU for trunk tissues (eg, BAT, white adipose tissue, vertebral bodies) in high load compared to no load. Other exploratory endpoints included changes in vital signs, total plasma cholesterol, plasma glucose, plasma insulin, plasma lactate, and plasma free fatty acids in high load compared with no load.

Statistical Analysis

Data analysis was performed using SPSS Statistics 29 (IBM Corp., Armonk, NY, USA). Normality of the data was explored using the Shapiro–Wilk test, which showed that variables for the primary endpoint and main secondary endpoints had normal distribution. The arithmetic mean values were calculated from the individual measurements and expressed at a precision of 1 SD (mean ± SD). To compare GU between interventions, paired samples *t*-tests were used. One-way ANOVA with Dunnett's post hoc test was used to compare the mean thoracic vertebral GU with the mean GU in the other 16 evaluated tissues [Supplementary Fig. S1 (28)]. *P*-values < .05 are considered statistically significant.

Results

Baseline Characteristics

A total of 10 men completed the trial according to the protocol and were included in the data analysis. Baseline characteristics from the screening visit for those participants are shown in Table 1.

GU Ratios Between Lower and Upper Extremity

According to the predefined primary outcome, GU ratios were calculated to compare GU in loaded and nonloaded regions of the body, ie, lower extremity (loaded) compared to upper extremity (nonloaded).

The GU ratio between loaded cortical bone and nonloaded cortical bone was increased in high load compared to no load; both the femur/humerus ratio (increased by 19%, $P = .029$) and the tibia/humerus ratio (increased by 18%, $P = .013$; Fig. 4A) were increased. Similarly, the GU ratio in the femur/humerus diaphyseal bone marrow regions was increased when comparing high load to no load (increased by 17%, $P = .041$; Fig. 4B). There was a tendency of increased GU ratio in the tibia/humerus diaphyseal bone marrow regions when comparing high load to no load ($P = .081$; Fig. 4B). The GU ratio in loaded muscle/nonloaded muscle was increased in high load compared to no load; both the m. quadriceps femoris/m. triceps brachii ratio (increased by 28%, $P = .014$) and the m. triceps surae/m. triceps brachii ratio (increased by 74%, $P = .011$; Fig. 4C) were increased. The GU ratio was not affected by increased loading when comparing SAT in the lower and upper extremities (Fig. 4D).

Absolute GU in Lower Extremities

In addition, absolute total GU (not adjusted for GU in upper extremities) was also significantly increased in muscles of the lower extremity, especially in triceps surae, with an increase of 8.2 $\mu mol \times kg^{-1\times} min^{-1}$ ($P = .02$) but also in quadriceps femoris with an increase of 2.3 $\mu mol \times kg^{-1\times} min^{-1}$ ($P = .02$) when comparing high load with no load [Supplementary Fig. S2 (28)]. No statistically significant effect of increased loading on absolute GU was observed in cortical bone, diaphyseal bone marrow, or SAT in the lower extremities [Supplementary Fig. S2 (28)]. However, there was a tendency of increased absolute GU in femoral cortical bone ($P = .07$) when comparing high load with no load [Supplementary Fig. S2 (28)].

GU in Trunk Region

Several different regions and tissues were analyzed in the trunk region to compare GU between high load and no load. No significant differences were observed in GU in the thoracic vertebral bodies, lumbar vertebral bodies, visceral adipose tissue, or SAT. There was a tendency ($P = .08$) toward lower GU in supraclavicular BAT during high load compared with no load [Supplementary Fig. S3 (28)].

Unexpectedly, the absolute GU in the vertebral bodies at both the thoracic (Th10-Th12) and the lumbar (L3-L5) levels were very high during both the no load and the high load treatments [Supplementary Fig. S3 (28)]. To relate GU in vertebraes to GU in other tissues, a comparison between GU in different tissues during the no load treatment was performed and is shown in Supplementary Fig. S1 (28). This demonstrates exceptionally high GU in the bone marrow of vertebral bodies, exceeding the GU in supraclavicular BAT and multiple skeletal muscles. GU in thoracic vertebral bodies was significantly higher compared to all other tissues except lumbar vertebral bodies. The highest absolute GU was observed in the bone marrow region of the vertebrae, followed by BAT and different skeletal muscles, followed by diaphyseal cortical bone, while the lowest GU was observed in adipose tissues [Supplementary Fig. S1 (28)].

Metabolic Plasma Markers

Glucose plasma levels were significantly increased 90 and 120 minutes after the intervention start during high load compared to no load. At 90 minutes, the high load glucose level was 5.4 mmol/L (± SD 0.3) compared to 5.2 mmol/L (± SD 0.3, $P = .003$) during no load. At 120 minutes, the high load glucose level was 5.5 mmol/L (± SD 0.3) compared to 5.3 mmol/L (± SD 0.4, $P = .006$) during no load (Fig. 5).

Insulin plasma levels were significantly increased 60 minutes after the intervention start during high load, 23 mU/L (± SD 11.0) compared to no load, 17.8 mU/L (± SD 6.9, $P = .018$). Lactate plasma levels were significantly increased at 180 minutes (the end of the intervention) during high load, 1.0 mmol/L (± SD 0.3) compared to no load, 0.8 mmol/L (± SD 0.2, $P = .03$). See Fig. 5.

No significant differences were observed in plasma levels of free fatty acids between no load and high load (Fig. 5).

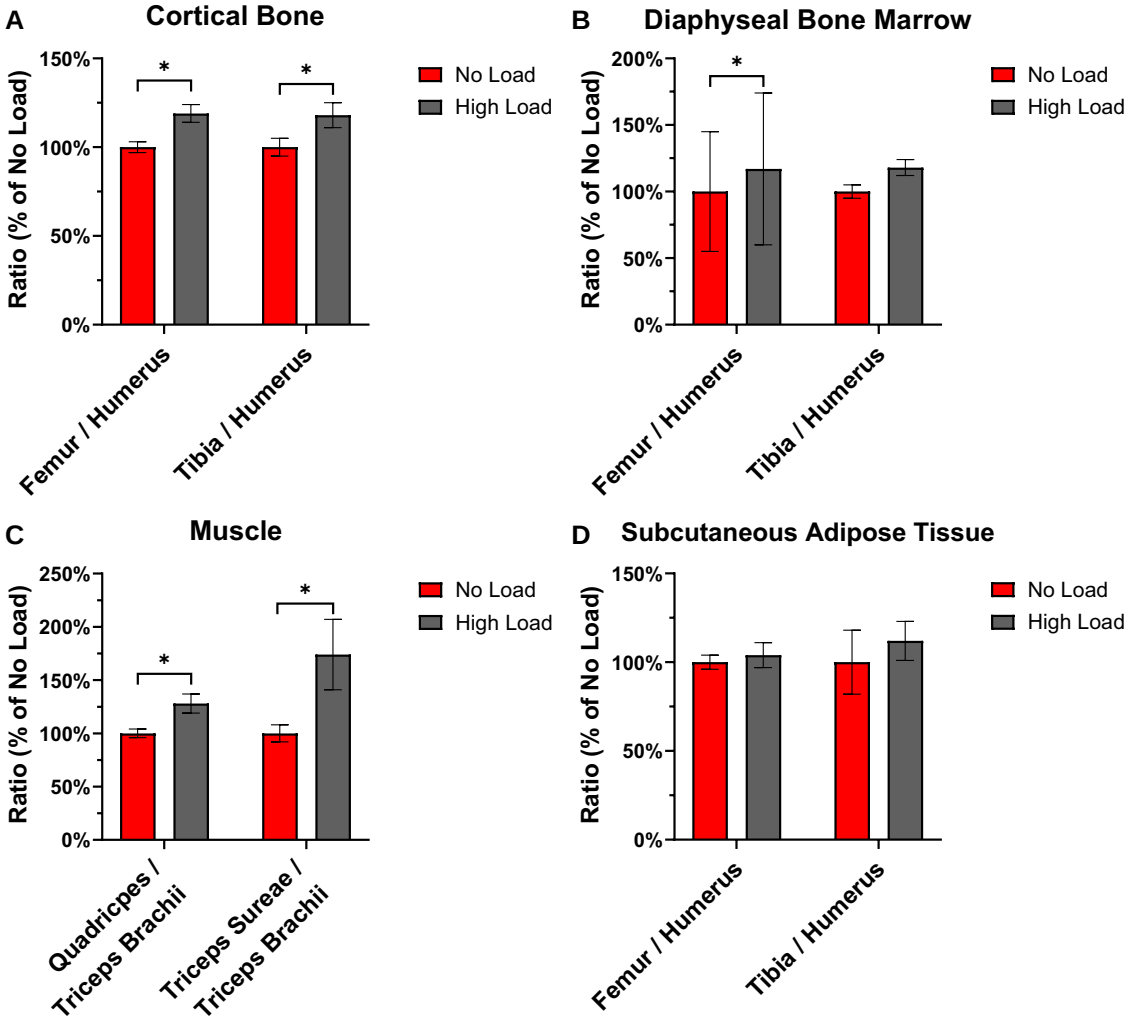

Figure 4. The effects of increased loading on the GU ratios between loaded extremities and not loaded extremities. (A) Cortical bone for femur/humerus GU ratio and tibia/humerus GU ratio. (B) Diaphyseal bone marrow region for femur/humerus GU ratio and tibia/humerus GU ratio. (C) Muscle for quadriceps/triceps brachii muscle GU ratio and triceps surae/triceps brachii muscle GU ratio. (D) SAT for femoral region SAT/humeral region SAT GU ratio and tibial region SAT/humeral region SAT GU ratio. Within group *P*-values (high load vs no load) are calculated using paired samples *t*-test. Data are expressed as mean ± SEM in percent of no load. * $P < .05$.

Abbreviations: GU, glucose uptake; SAT, subcutaneous adipose tissue.

Pulse and Blood Pressure

Pulse and diastolic blood pressure were significantly increased 90 and 180 minutes after the start of the intervention during high load compared to no load. Pulse at 90 minutes was 87 beats per minute (bpm; ± SD 11.4) during high load and 68 bpm (± SD 10.3, $P < .001$) during no load. Pulse at 180 minutes was 85 bpm (± SD 12.2) during high load and 68 bpm (± SD 9.3, $P = .002$) during no load (Fig. 6).

Diastolic blood pressure at 90 minutes was 98 mmHg (± SD 13.8) during high load and 88 mmHg (± SD 23.3, $P = .001$) during no load. Diastolic blood pressure at 180 minutes was 97 mmHg (± SD 10.7) during high load and 88 mmHg (± SD 10.0, $P = .003$) during no load (Fig. 6).

No significant differences were seen in systolic blood pressure between the 2 treatments (Fig. 6).

Discussion

Studies have reported associations between increased standing time and improved health as well as improved insulin sensitivity (2). Furthermore, it has been demonstrated that standing increases overall energy expenditure, which could help prevent weight gain even if the magnitude of increase may not be large enough to make standing an effective treatment for obesity (29). However, in addition to standing, it has been proposed that increased weight-bearing loading reduces body weight and body fat mass via a homoeostatic mechanism (30). In this study, we demonstrate that glucose metabolism in muscle and bone is influenced by increased weight-bearing loading achieved by changing posture from sitting (no load) to standing with a weight vest (high load).

Although it is well established that dynamic exercise increases GU in exposed muscles (18, 31), it was unknown if static loading achieved by wearing an exogenous weight during standing affects GU locally in bone and/or muscle in the lower extremities. In this trial, we combine standing with increased weight-bearing loading by adding weight vests to maximize the loading difference between treatments to better evaluate the effects of increased loading in addition to the effects of standing. We show that increased weight-bearing

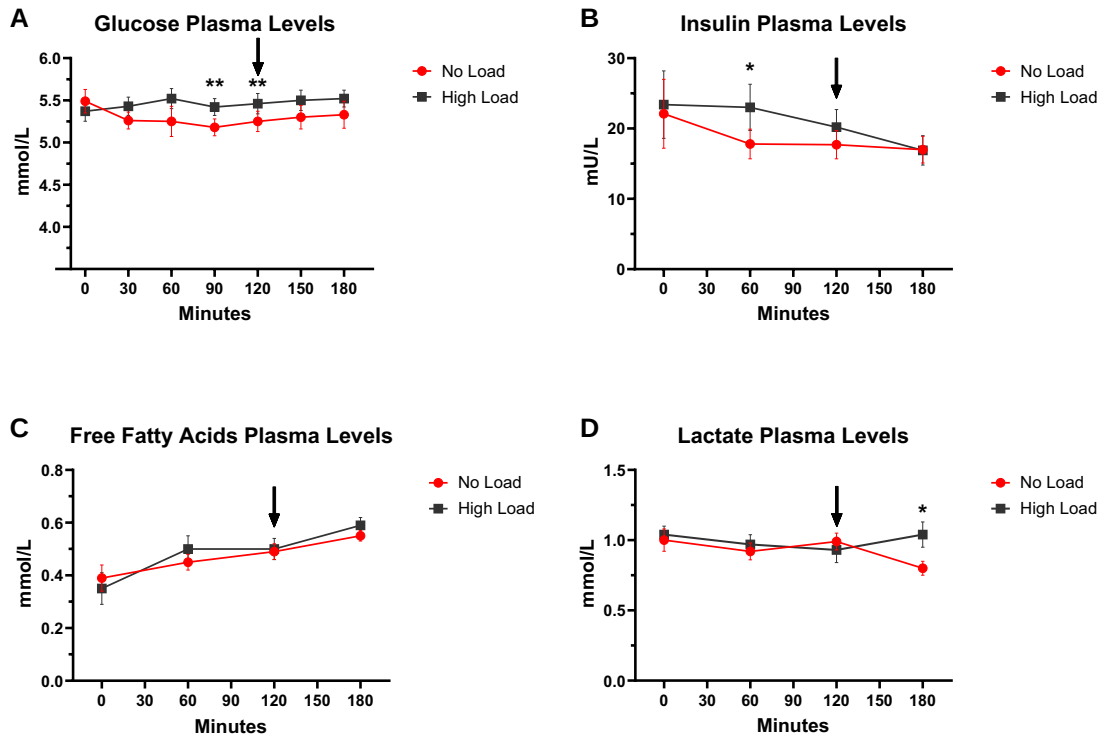

Figure 5. Effect of increased loading on plasma levels of metabolic markers. Increased loading significantly increases (A) glucose levels at 90 and 120 minutes, (B) insulin levels at 60 minutes, and (D) lactate levels at 180 minutes. No significant difference between no load and high load for free fatty acids (C). Black arrows at 120 minutes represent timepoint of ^{18}F-FDG injection. Data are expressed as mean ± SEM. $*P < .05$, $**P < .01$.
Abbreviations: ^{18}F-FDG, 2-deoxy-2-[^{18}F]-fluoro-D-glucose.

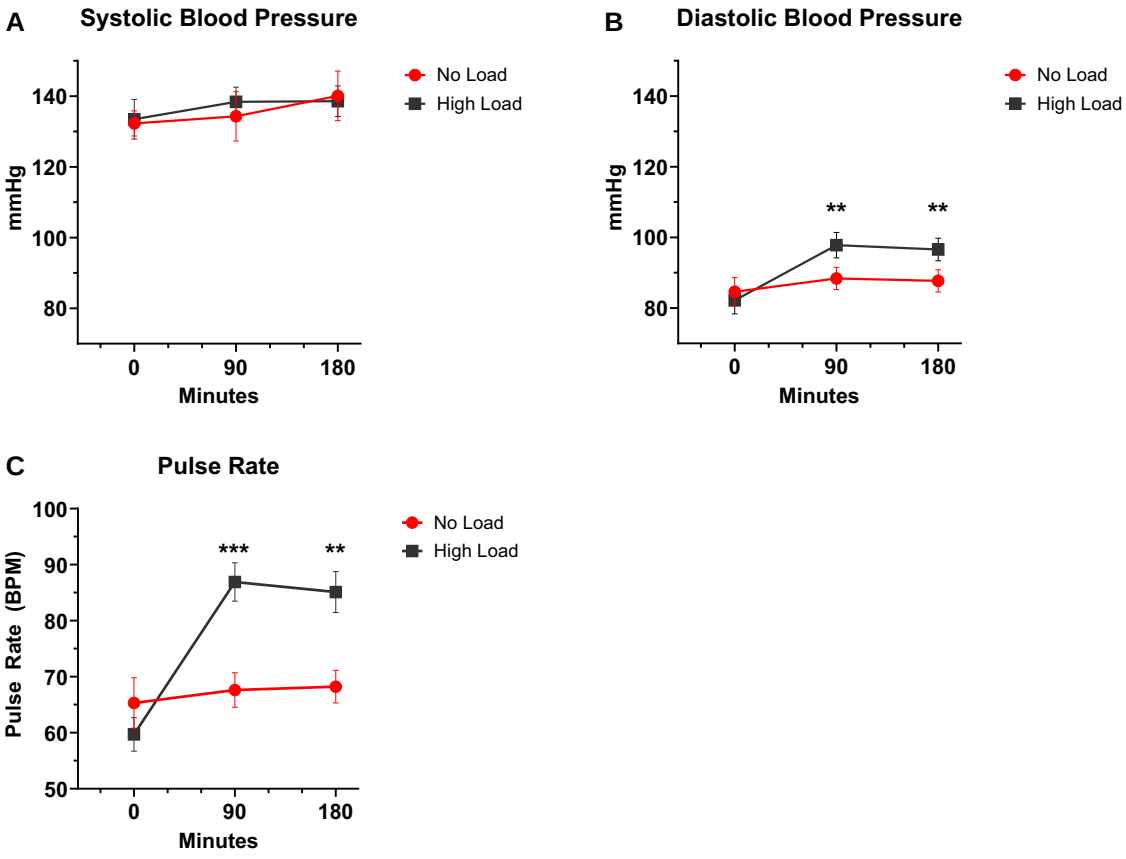

Figure 6. Effect of increased loading on vital parameters. No significant difference between no load and high load for systolic blood pressure (A). Increased loading significantly increases (B) diastolic blood pressure and (C) pulse at 90 and 120 minutes. Data are expressed as mean ± SEM. $**P < .01$, $***P < .001$.

loading increases GU in cortical bone, bone marrow, and muscles in the exposed regions of the lower extremities.

It has not previously been shown that increased weight-bearing loading increases GU in cortical bone. Our present findings suggest that the cortical bone responds to increased loading with enhanced GU to account for increased energy demand from bone remodeling due to augmented loading-induced strain in the bone tissue. This would then implicate an increased local energy expenditure, caused by loading and dependent on gravitational forces (30). The main glucose transporter (GLUT) in osteoprogenitor cells is thought to be the insulin-independent GLUT1, but the insulin-dependent GLUT4 may also play a role, as it does in skeletal muscles (32, 33). In this study, we cannot determine which glucose transporter mediates the GU, but we propose that it may be the insulin-independent GLUT1, since there was no difference in plasma insulin levels between treatments after ^{18}F-FDG injection.

We observed a loading-induced increase of the femur/humerus GU ratio not only in the cortical bone but also in the bone marrow region. It has previously been demonstrated that bone marrow metabolism differs depending on anatomical location and is impaired in insulin resistance. GU and insulin sensitivity appears to be improved in femoral bone marrow after exercise while it is not affected in vertebral bone marrow (34, 35). GU in vertebral bone marrow has been shown not to be affected by insulin stimulation, and it appears to be lower in individuals suffering from obesity and diabetes compared to the nonobese without diabetes (36). This indicates that femoral bone marrow is an insulin-sensitive tissue while vertebral bone marrow may not be insulin sensitive. At present, the results are, however, a bit conflicting, and further studies are warranted to elucidate the mechanism for GU regulation in vertebral bone marrow (37). A previous study has demonstrated that the GU in bone marrow is not completely linked to exercise and the GU of muscles (18), indicating that the increase in GU ratio for bone marrow in the present study could be a direct effect, not only mediated via increased muscle activation. Bone marrow is an active tissue that has many physiological functions locally and possibly at the systemic level (36, 38). Consequently, the present findings may have important implications in understanding the role of bone marrow in metabolic disorders and glucose metabolism.

The observed loading-induced increase in muscle GU was expected as the change in posture activates postural muscles to maintain an upright position, which in turn generates an increase in energy demand. It has previously been demonstrated that GU in skeletal muscles in general is lower in individuals with obesity compared to lean individuals, which is believed to be caused by reduced insulin sensitivity (39). Previous studies have shown that active exercise increases GU in muscles (18, 19). However, the present study is the first to demonstrate that standing, resulting in static muscle activation, indeed increases GU in postural muscles, especially in the lower part of the leg (triceps surae muscle). This is probably a sign of increased energy demand, which could be one of the factors relating standing to improved health, for example, improved insulin sensitivity (2).

In a recent cross-sectional study, it was observed that high BMI was associated with high GU of the long bones in the lower extremities (40). This previous observational finding is in line with the present functional study demonstrating that increased loading enhances GU in the weight-bearing skeleton in the lower extremities. The relationship between increased loading or obesity and bone is complex. Obesity has numerous effects on bone metabolism, including fat accumulation, enhanced bone formation, and secretion of proinflammatory cytokines (41, 42). Bones exposed to increased loading may require more energy to increase bone mass and maintain bone balance to support the heavier body. The increased GU in cortical bone and bone marrow may also indicate crosstalk between bone and systemic glucose homeostasis.

The increased diastolic blood pressure and pulse rate observed in the present study are most likely caused by the posture change since diastolic blood pressure, peripheral resistance, and the pulse rate are known to increase when standing. Cardiac output and stroke volume still decrease when standing, maybe as a consequence of a decreased central blood pool (43, 44).

Despite the increased GU by various tissues during the high load treatment, the blood glucose and insulin levels stayed the same or even increased compared to the no load treatment (Fig. 5). This might be due to compensatory increased glucose production from the liver. The increase in plasma glucose levels by increased weight-bearing loading that were observed at 90 and 120 minutes after treatment start could be attributed to physiological changes from, for example, increased pulse rate or a systemic increase in energy demand. This could be caused in part by muscle activation but possibly also by increased glucose demand from cortical bone and/or bone marrow generating a systemic stress response causing increased gluconeogenesis and glycogenolysis. The difference in insulin levels at 60 minutes is probably caused by the preceding positive slope of the plasma glucose levels during high load, stimulating insulin release from pancreatic beta cells. Another possible explanation for the increase of insulin and glucose levels during high load is that increased sympathetic tone while standing with a weight vest induced a transient increase in insulin and glucagon secretion (45). Interestingly, we also observed that increased weight-bearing loading increased plasma lactate levels at the end of the treatment. The lactate increase could be due to anaerobic metabolism caused by skeletal muscle fatigue or hypoxia even though this is unlikely due to the low intensity workload of the treatments combined with the high capacity of muscle cells for aerobic metabolism (46). It is possible that the increased lactate from increased weight-loading is due to a general increase of GU in peripheral tissues other than muscle cells such as bone marrow, which have a lower aerobic metabolic potential to metabolize lactate, resulting in an increase of lactate release into the bloodstream.

An unexpected finding in the present study was the exceptionally high GU in the bone marrow region of the vertebral bodies that was independent of the loading. The GU in the vertebral bone marrow region was even higher than in supraclavicular BAT and in skeletal muscles, 2 tissues known to have very high GU (34, 47). Evidence suggests that vertebral bone marrow differs from femoral and tibial bone marrow, with the vertebrae consisting of more red marrow and less BMAT while the bone marrow of the long bones consists of more BMAT (37, 38). It is well established that the main function of the vertebral body bone marrow is hematopoiesis. In addition, we propose that the vertebral bone marrow region might be involved in systemic glucose homeostasis. Previous studies suggest that femoral bone marrow insulin sensitivity correlates with whole-body insulin sensitivity and that

exercise increases femoral bone marrow insulin sensitivity but not vertebral bone marrow insulin sensitivity (34, 35). Another recent study showcased aligning results with high GU in vertebral bone marrow. The authors also showed that GU increases in femur, tibia, and fibula in correlation with increased BMI, while no correlation was shown between BMI and GU of the vertebrae (40). Further studies should determine the role of the vertebral bone marrow region for systemic glucose homeostasis, including studies that determine whether the GU in the vertebral bone marrow region is regulated by factors known to regulate GU and/or insulin resistance in muscle and/or white adipose tissue.

Strengths of the present pilot study include the use of state-of-the art whole-body PET study-based analyses and the crossover design, comparing 2 different loading protocols in the same subjects. Limitations of the present study design include difficulties in separating the loading effect per se from the effects of the postural changes and corresponding muscle activation. To investigate this, another intervention consisting of standing without a weight vest should have been included. It would also be of interest to investigate how GU responds to different levels of weight-bearing loading. Other limitations are that only men were included, the duration of the intervention was short, and physical activity was not measured. The design with standing and adding a weight vest was chosen to maximize the difference in loading between the 2 interventions: (1) standing with a vest and (2) sitting without a vest. A predefined ratio was used as a primary endpoint to look at GU in loaded tissues vs nonloaded tissues to achieve increased specificity on local effects. The sample size ($n = 10$) was relatively small in the present study, and we may, therefore, not have detected true effects of minor magnitude. Participants in this study were insulin resistant, according to the homeostatic model assessment for insulin resistance index, with a mean value of 4.2 ($\pm$ SD 1.9) at screening. It is unclear if or how this insulin resistance could have affected the results. Future studies are warranted to further investigate the systemic effects on energy expenditure and to separate the weight-bearing loading effect from the effects of standing. Future, more comprehensive studies should include larger sample sizes including both men and women.

In conclusion, increased weight-bearing loading enhances GU in muscles, cortical bone, and bone marrow in the exposed lower extremities. This could be interpreted as increased local energy demand in bone and muscle caused by increased loading and/or the static workload of standing. The physiological importance of the increased local GU by static loading remains to be determined, but these results indicate potential positive health effects from standing and increased weight-bearing loading. Further studies should determine the nature of the unexpected very high GU in vertebral bodies.

Acknowledgments

The study was conducted as a collaboration between the University of Gothenburg, Sweden, which initiated the study, and Turku PET Centre, University of Turku, Finland, where the study was performed. The authors thank the contribution of the personnel of the Turku PET Centre for their excellent assistance during the study and the participants who participated in the study. Fig. 2 was created with publication rights from BioRender.com.

Funding

Supported with grants from the Knut and Alice Wallenberg Foundation (KAW 2020.0230), the Torsten Söderberg Foundation (MT 3/20), and the Göteborgs Läkaresällskap (22/972547).

Author Contributions

Conceptualization, J.B., C.O., PA.J., and JO.J.; Methodology, J.B., C.O., PA.J., D.H., K.K., A.R., and P.N.; Access to all data, J.B., A.R., and K.K.; Formal Analysis, J.B. and T.S.; Investigation, J.B., T.S., A.R., K.K., and E.A.H.; Resources, J.H., O.E., and K.K. Writing—Original Draft, J.B. and C.O.; Writing—Review & Editing, J.B., T.S., D.H., E.A.H., K.L., P.N., JO.J, PA.J., K.K, A.R., and C.O.; Visualization, J.B., C.O., and PA.J.; Supervision, C.O., PA.J., K.K., A.R., and P.N.; Funding Acquisition, C.O. and A.R.; Approval final manuscript, J.B., T.S., D.H., E.A.H., J.H., O.E., K.L., P.N., JO.J., PA.J., K.K., A.R., and C.O.

Disclosures

The authors have nothing to disclose.

Data Availability

Restrictions apply to the availability of the data generated or analyzed during this study to preserve patient confidentiality. The corresponding author will on request detail the restrictions and any conditions under which access to some data may be provided.

Clinical Trial Information

ClinicalTrials.gov ID: NCT05443620

References

1. Tsao CW, Aday AW, Almarzooq ZI, *et al.* Heart disease and stroke statistics-2023 update: a report from the American Heart Association. *Circulation*. 2023;147(8):e93-e621.
2. Garthwaite T, Sjoros T, Koivumaki M, *et al.* Standing is associated with insulin sensitivity in adults with metabolic syndrome. *J Sci Med Sport*. 2021;24(12):1255-1260.
3. Husu P, Suni J, Tokola K, *et al.* Frequent sit-to-stand transitions and several short standing periods measured by hip-worn accelerometer are associated with smaller waist circumference among adults. *J Sports Sci*. 2019;37(16):1840-1848.
4. Shuval K, Barlow CE, Finley CE, Gabriel KP, Schmidt MD, DeFina LF. Standing, obesity, and metabolic syndrome: findings from the Cooper Center longitudinal study. *Mayo Clin Proc*. 2015;90(11):1524-1532.
5. Levine JA, Lanningham-Foster LM, McCrady SK, *et al.* Interindividual variation in posture allocation: possible role in human obesity. *Science*. 2005;307(5709):584-586.
6. Jansson JO, Palsdottir V, Hagg DA, *et al.* Body weight homeostat that regulates fat mass independently of leptin in rats and mice. *Proc Natl Acad Sci U S A*. 2018;115(2):427-432.
7. Ohlsson C, Gidestrand E, Bellman J, *et al.* Increased weight loading reduces body weight and body fat in obese subjects—a proof of concept randomized clinical trial. *EClinicalMedicine*. 2020;22:100338.
8. Guntur AR, Rosen CJ. Bone as an endocrine organ. *Endocr Pract*. 2012;18(5):758-762.
9. Etherington J, Harris PA, Nandra D, *et al.* The effect of weight-bearing exercise on bone mineral density: a study of female ex-elite

athletes and the general population. *J Bone Miner Res*. 1996;11(9):1333-1338.
10. Pagnotti GM, Styner M, Uzer G, *et al*. Combating osteoporosis and obesity with exercise: leveraging cell mechanosensitivity. *Nat Rev Endocrinol*. 2019;15(6):339-355.
11. Hägg D, Jansson P-A, Bellman J, Jansson J-O, Ohlsson C. Osteoblast-lineage cells regulate metabolism and fat mass. *Curr Opin Endocr Metab Res*. 2023;31:100470.
12. Scheller EL, Rosen CJ. What's the matter with MAT? Marrow adipose tissue, metabolism, and skeletal health. *Ann N Y Acad Sci*. 2014;1311(1):14-30.
13. Scheller EL, Cawthorn WP, Burr AA, Horowitz MC, MacDougald OA. Marrow adipose tissue: trimming the fat. *Trends Endocrinol Metab*. 2016;27(6):392-403.
14. Cipriani C, Colangelo L, Santori R, *et al*. The interplay between bone and glucose metabolism. *Front Endocrinol (Lausanne)*. 2020;11:122.
15. Karner CM, Long F. Glucose metabolism in bone. *Bone*. 2018;115:2-7.
16. Lecka-Czernik B. Marrow fat metabolism is linked to the systemic energy metabolism. *Bone*. 2012;50(2):534-539.
17. Cawthorn WP, Scheller EL, Learman BS, *et al*. Bone marrow adipose tissue is an endocrine organ that contributes to increased circulating adiponectin during caloric restriction. *Cell Metab*. 2014;20(2):368-375.
18. Heinonen I, Kemppainen J, Fujimoto T, Knuuti J, Kalliokoski KK. Increase of glucose uptake in human bone marrow with increasing exercise intensity. *Int J Sport Nutr Exerc Metab*. 2019;29(3):254-258.
19. Heinonen I, Kemppainen J, Kaskinoro K, *et al*. Bone blood flow and metabolism in humans: effect of muscular exercise and other physiological perturbations. *J Bone Miner Res*. 2013;28(5):1068-1074.
20. Rudroff T, Kindred JH, Kalliokoski KK. [18f]-FDG positron emission tomography–an established clinical tool opening a new window into exercise physiology. *J Appl Physiol (1985)*. 2015;118(10):1181-1190.
21. Ishizu KYY. Clarification of a fractional uptake concept—reply. *The Journal of Nuclear Medicine*. 1995;36:712.
22. Thie JA. Clarification of a fractional uptake concept. *J Nucl Med*. 1995;36(4):711-712.
23. Peltoniemi P, Lönnroth P, Laine H, *et al*. Lumped constant for [18F] fluorodeoxyglucose in skeletal muscles of obese and nonobese humans. *Am J Physiol Endocrinol Metab*. 2000;279(5):E1122-E1130.
24. Virtanen KA, Peltoniemi P, Marjamäki P, *et al*. Human adipose tissue glucose uptake determined using [18F]-fluoro-deoxy-glucose ([18F]FDG) and PET in combination with microdialysis. *Diabetologia*. 2001;44(12):2171-2179.
25. Snyder W. Chapter 2: Gross and elemental content of reference man. In: *Report of the Task Group on Reference Man*. Annals of the ICRP/ICRP Publication Vol. 23. Pergamon Press; 1975:273-334.
26. Manley SE, Hikin LJ, Round RA, *et al*. Comparison of IFCC-calibrated HbA1c from laboratory and point of care testing systems. *Diabetes Res Clin Pract*. 2014;105(3):364-372.
27. Matthews DR, Hosker JP, Rudenski AS, Naylor BA, Treacher DF, Turner RC. Homeostasis model assessment: insulin resistance and?-cell function from fasting plasma glucose and insulin concentrations in man. *Diabetologia*. 1985;28(7):412-419.
28. Bellman J, Sjöros T, Hägg D, *et al*. Supplemental Materials for "Loading enhances glucose uptake in muscles, bones, and bone marrow of lower extremities in humans". *Zenodo*. https://doi.org/10.5281/zenodo.11083143. Deposited 29 April 2024.
29. BETTS JA, SMITH HA, JOHNSON-BONSON DA, *et al*. The energy cost of sitting versus standing naturally in man. *Med Sci Sports Exerc*. 2019;51(4):726-733.
30. Jansson J-O, Anesten F, Hägg D, *et al*. The dual hypothesis of homeostatic body weight regulation, including gravity-dependent and leptin dependent actions. *Phil Trans R Soc*. 2023;378(1888):20220219.
31. Fujimoto T, Kemppainen J, Kalliokoski KK, Nuutila P, Ito M, Knuuti J. Skeletal muscle glucose uptake response to exercise in trained and untrained men. *Med Sci Sports Exerc*. 2003;35(5):777-783.
32. Wei J, Shimazu J, Munevver, *et al*. Glucose uptake and runx2 synergize to orchestrate osteoblast differentiation and bone formation. *Cell*. 2015;161(7):1576-1591.
33. Dixit M, Liu Z, Poudel SB, *et al*. Skeletal response to insulin in the naturally occurring type 1 diabetes Mellitus mouse model. *JBMR Plus*. 2021;5(5):e10483.
34. Ojala R, Motiani KK, Ivaska KK, *et al*. Bone marrow metabolism is impaired in insulin resistance and improves after exercise training. *J Clin Endocrinol Metab*. 2020;105(12):e4290-e4303.
35. Huovinen V, Bucci M, Lipponen H, *et al*. Femoral bone marrow insulin sensitivity is increased by resistance training in elderly female offspring of overweight and obese mothers. *PLoS One*. 2016;11(9):e0163723.
36. Pham TT, Ivaska KK, Hannukainen JC, *et al*. Human bone marrow adipose tissue is a metabolically active and insulin-sensitive distinct fat depot. *J Clin Endocrinol Metab*. 2020;105(7):2300-2310.
37. Huovinen V, Saunavaara V, Kiviranta R, *et al*. Vertebral bone marrow glucose uptake is inversely associated with bone marrow fat in diabetic and healthy pigs: [(18)F]FDG-PET and MRI study. *Bone*. 2014;61:33-38.
38. Suchacki KJ, Tavares AAS, Mattiucci D, *et al*. Bone marrow adipose tissue is a unique adipose subtype with distinct roles in glucose homeostasis. *Nat Commun*. 2020;11(1):3097.
39. Koh H-CE, van Vliet S, Meyer GA, *et al*. Heterogeneity in insulin-stimulated glucose uptake among different muscle groups in healthy lean people and people with obesity. *Diabetologia*. 2021;64(5):1158-1168.
40. Lu W, Duan Y, Li K, Qiu J, Cheng Z. Glucose uptake and distribution across the human skeleton using state-of-the-art total-body PET/CT. *Bone Res*. 2023;11(1):36.
41. Hou J, He C, He W, Yang M, Luo X, Li C. Obesity and bone health: a Complex link. *Front Cell Dev Biol*. 2020;8:600181.
42. Cao JJ. Effects of obesity on bone metabolism. *J Orthop Surg Res*. 2011;6(1):30.
43. Olufsen MS, Ottesen JT, Tran HT, Ellwein LM, Lipsitz LA, Novak V. Blood pressure and blood flow variation during postural change from sitting to standing: model development and validation. *J Appl Physiol Respir Environ Exerc Physiol*. 2005;99(4):1523-1537.
44. Ganong WF. *Review of Medical Physiology*. McGraw Hill; 2019.
45. Rorsman P, Ashcroft FM. Pancreatic β-cell electrical activity and insulin secretion: of mice and men. *Physiol Rev*. 2018;98(1):117-214.
46. Ferguson BS, Rogatzki MJ, Goodwin ML, Kane DA, Rightmire Z, Gladden LB. Lactate metabolism: historical context, prior misinterpretations, and current understanding. *Eur J Appl Physiol*. 2018;118(4):691-728.
47. Virtanen KA, Lidell ME, Orava J, *et al*. Functional brown adipose tissue in healthy adults. *N Engl J Med*. 2009;360(15):1518-1525.